Available online at www.sciencedirect.com
ScienceDirect
Computers & Graphics 32 (2008) 116–119
COMPUTERS & GRAPHICS
www.elsevier.com/locate/cag

Chaos and Graphics

Chaotic pattern of unsmoothed isochromatics around the regions of concentrated stresses

Minvydas Ragulskis[a,*], Miguel A.F. Sanjuan[b]

[a]Research Group for Mathematical and Numerical Analysis of Dynamical Systems, Department of Fundamental Sciences, Kaunas University of Technology, Studentu 50-222, Kaunas LT-51638, Lithuania
[b]Nonlinear Dynamics and Chaos Group, Departamento de Fisica, Universidad Rey Juan Carlos, Mostoles, 28933 Madrid, Spain

Abstract

Photoelastic isochromatics are computationally reconstructed from the results of finite element analysis. Fast variation of the components of stresses cannot be approximated by a coarse non-adaptive finite element mesh. Visually chaotic and attractive looking pattern of numerically reconstructed photoelastic fringes prevents interpretation of the field of stresses around the regions of concentrated stresses. The phrase "chaotic pattern" is used in this paper in a loose sense to refer to the intricate and unpredictable patterns produced by this approach. One goal of this paper is to present these photoelastic patterns for their aesthetic appeal.

Keywords: Photoelasticity; Finite elements; Chaos

1. Introduction

Computational mechanics is a fundamental part of computational science and engineering and is concerned with the use of computational techniques to characterise, predict, and simulate physical events and engineering systems governed by the laws of mechanics. Research in computational mechanics is usually interdisciplinary in nature, reflecting a combination of concepts, methods, and principles that often span several areas of mechanics, mathematics, computer sciences and other scientific disciplines as well [1].

Hybrid numerical–experimental analysis techniques are widely used in computational and experimental mechanics [2]. Such techniques have seen limited applications during the 1970s, but have been revived with the vastly improved modern computational technology. By introducing the experimental results as initial and boundary conditions, modern computer codes can be used to yield results which are unobtainable when only one of the two techniques is used. The hybrid techniques thus exemplify the complementary role of the experimental and numerical techniques especially in such areas as mechanical stress analysis [3,4].

Photoelasticity is one of the oldest methods for experimental stress analysis, but has been overshadowed by the finite element method (FEM) for engineering applications over the past three decades [5]. However, new developments and applications, such as infrared photoelasticity, low-cost dynamic photoelasticity, photoelastic applications in stereoreolitography, etc., have revived the use of experimental photoelasticity [6,7]. Thus, computational mimicking of patterns of photoelastic fringes becomes an important part of hybrid stress analysis techniques.

Unfortunately, conventional FEM techniques are based on the approximation of nodal displacements (not stresses) via the shape functions [8] whereas the formation of photoelastic fringes is governed by the distribution of stresses. Many engineering problems comprise concentrated stresses; therefore production of smooth patterns of photoelastic fringes would require unrealistically dense meshing. Ramesh and Pathak [9] have correctly noted that photoelastic isochromatics can be effectively used for the detection of FEM meshing problems. Photoelastic fringes become unsmooth and accurate numerical reconstruction

*Corresponding author.
E-mail addresses: minvydas.ragulskis@ktu.lt (M. Ragulskis), miguel.sanjuan@urjc.es (M.A.F. Sanjuan).

0097-8493/$ - see front matter © 2007 Elsevier Ltd. All rights reserved.
doi:10.1016/j.cag.2007.09.004

of the experimental pattern of photoelastic isochromatics becomes very complicated around the regions of concentrated stresses. Adaptive FEM meshing, computational smoothing of stress fields are common procedures used in hybrid numerical–experimental techniques for realistic visualisation of photoelastic patterns. Instead we will use a non-adaptive FEM mesh and will focus on the beauty of the photoelastic isochromatics around the regions of concentrated stresses because the main goal of this paper is to present these photoelastic patterns for their aesthetic appeal.

2. Construction of digital phototoelastic images

A two-dimensional static stress problem is considered. A FEM model yields the following relationship between the nodal displacements and stress fields [8]:

$$\begin{Bmatrix} \sigma_x(x,y) \\ \sigma_y(x,y) \\ \tau_{xy}(x,y) \end{Bmatrix} = [D][B]\{\delta\}, \tag{1}$$

where σ_x, σ_y and τ_{xy} are the components of the stresses in the problem of plain stress; $[B]$ is the matrix relating the strains with the displacements; $[D]$ is the matrix relating the stresses with the strains; $\{\delta\}$ is the vector of nodal displacements. Matrix $[B]$ is comprised from partial derivatives of the shape functions, which are used to interpolate nodal displacements in the domain of every finite element. Therefore, stress fields are continuous in the domains of every finite element, but discontinuous at inter-element boundaries of FEM mesh due to the operation of differentiation.

The procedure of conjugate approximation [8] yields the following algebraic system of equations for the determination of nodal values of stress:

$$\iint_{GS} [N]^{\mathrm{T}}[N]\,\mathrm{d}x\,\mathrm{d}y\,\{S_i\} = \iint_{GS} [N]^{\mathrm{T}}\sigma_i(x,y)\,\mathrm{d}x\,\mathrm{d}y, \tag{2}$$

where $[N]$ is the row vector of the shape functions of the current finite element; σ_i is the ith component of the stresses ($i = 1,2,3$); $\{S_i\}$ is the vector of smoothed nodal values of the smoothed component of the stresses in the global domain; GS stands for the procedure of global stiffness [8] (assembly of local elements to the global FEM matrixes).

When the vector of nodal values of stresses $\{S_i\}$ is solved from Eq. (2), the smoothed field of stresses is again interpolated in the domain of every finite element using its shape functions. Then, the principal stresses σ_a and σ_b are calculated as the eigenvalues of the matrix $\begin{bmatrix} \sigma_x & \tau_{xy} \\ \tau_{xy} & \sigma_y \end{bmatrix}$ at any point in the global domain [5]. We use monochromatic light for a better definition of the fringes, especially in areas with dense fringes as at stress concentration points. The greyscale intensity of the photoelastic image for the circular polariscope (isochromatics) is calculated as

$$I(x,y) = (\sin\, C(\sigma_a(x,y) - \sigma_b(x,y)))^2, \tag{3}$$

where C is the constant dependant on the thickness of the analysed structure in the state of plane stress and on the material from which it is produced [5]. The plotting algorithm used to visualise the results of calculations is independent from the physical model of the system and is described in detail in [10].

3. Computational experiments

A model of a plane disk in diametral compression is a paradigm in experimental stress analysis [2]. We use this model to illustrate the beauty and complexity of photoelastic isochromatics around the regions of concentrated stresses.

One-quarter of the disk is analysed; FEM meshes in the state of equilibrium and in the deformed state are presented in Fig. 1a. It is assumed that a flat not-deformable boundary presses the top part of the quarter disk. The degree of freedom of the nodes at the bottom of

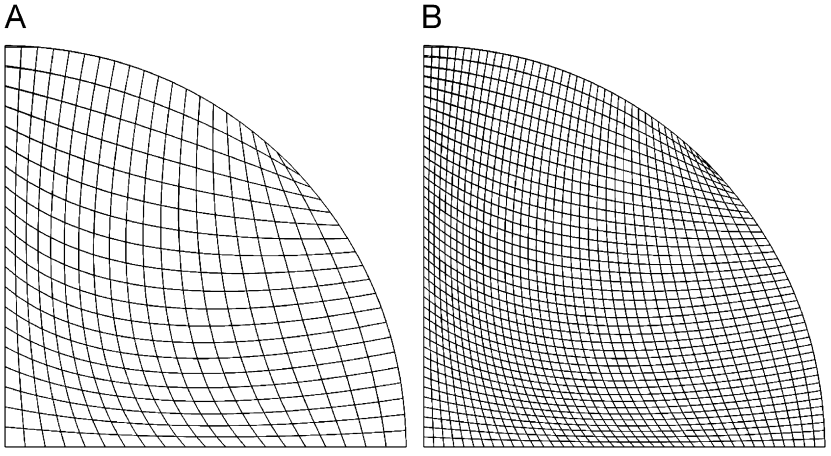

Fig. 1. Finite element mesh of a quarter of the disk: (A) 100 finite elements and (B) 400 finite elements.

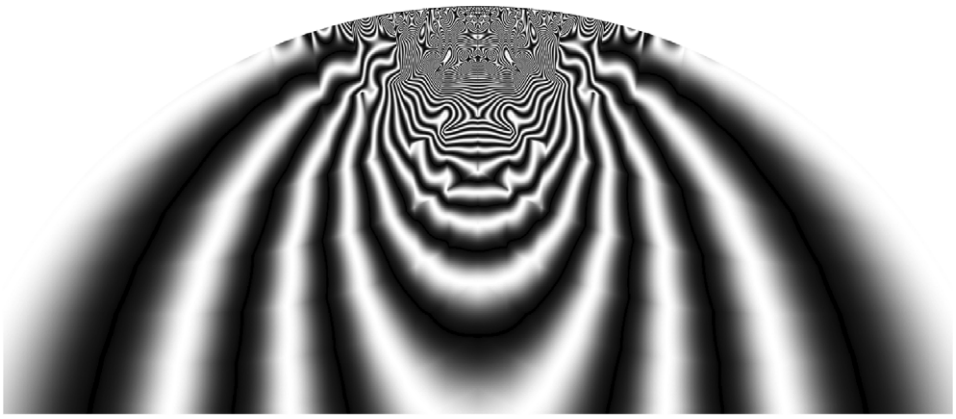

Fig. 2. Pattern of photoelastic isochromatics representing disk in diametral compression at $C = 300$.

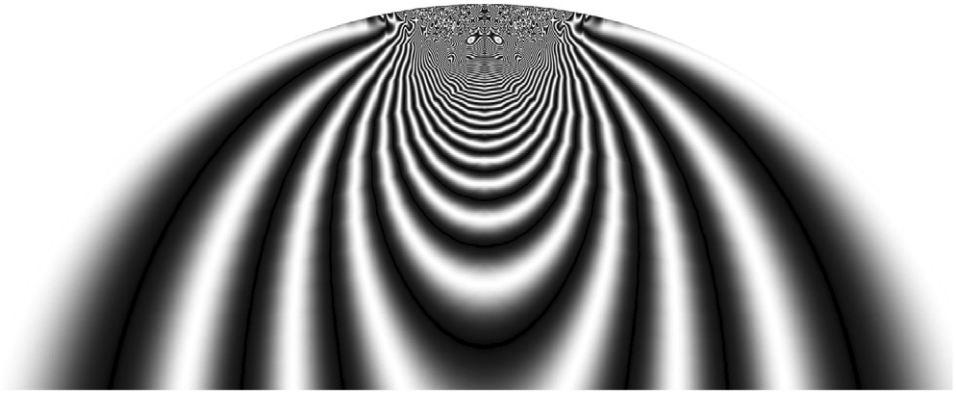

Fig. 3. Pattern of photoelastic isochromatics produced by doubly dense mesh.

the quarter disk has zero displacement in vertical direction and the degree of freedom of the nodes along the vertical edge of the quarter of disk has zero displacement in horizontal direction. First, static elastic equilibrium problem is solved and nodal displacements from the state of equilibrium are calculated. Then, previously described conjugate approximation is used to reconstruct nodal values of stresses and, finally, photoelastic isochromatics are plotted.

Two symmetric disk quarters are used to visualise the area around the contact. It is clear that concentrated stresses subjacent to the contact plane require a meshing with vanishing elements at the contact point for exact representation of the stress field. The pattern of isochromatics is refracted at inter-element boundaries which is a mark of problems associated with meshing (Fig. 2). It is naïve to expect that non-adaptive FEM mesh can reproduce satisfactory results around singular points.

Visually chaotic pattern of fringes is generated around the contact area and compromise the physical interpretation of this pattern. Thick isochromatics at the bottom part of the image (Fig. 2) provide a nice illustration of the variation of the stress field in that area. One could expect to see a similar pattern of experimental photoelastic fringes for a disk in diametral compression [2]. But the picture becomes not interpretable around the region of concentrated stresses. Computational "tools" used to measure the fast variation of the physical quantity are simply too "rough".

In order to illustrate the unpredictability of this visually chaotic pattern of fringes around the contact area we repeat the computational experiment with a doubly dense mesh (all other parameters, including the value of constant C are kept the same). Hundred Lagrange nine node finite elements are used to construct the mesh for the disk quarter (Fig. 1a). The doubly dense mesh comprises 400 finite elements (it is also a non-adaptive mesh) and is shown in Fig. 1b; the produced pattern of isochromatics is presented in Fig. 3. The fringes at the bottom part of Fig. 3 are smooth and nice. One can still observe some slight fringe discontinuities in the middle part of the image, but the number of properly reconstructed fringes is much higher compared to Fig. 2. Nevertheless, doubly dense mesh does not help to improve the pattern of fringes around the regions of concentrated stress. The zone of unphysical behaviour of photoelastic fringes is smaller in Fig. 3 compared to Fig. 2, but visual stochasticity of the photoelastic pattern is not less there. Moreover, the chaotic fringe patterns in Figs. 2 and 3 are not similar. That is a definite sign of the unpredictability of the distribution of photoelastic fringes around the regions of concentrated stresses.

The readers can rather easily reproduce the greyscale pattern of photoelastic isochromatics. Of course, one must use FEM software to calculate nodal displacements from the state of equilibrium. This is a basic step of FEM analysis. Then, one needs to calculate nodal stresses. This is also an ordinary feature of standard FEM packages. Otherwise, one needs to solve the system of algebraic equations defined in Eq. (2). Then, the nodal values of stresses (σ_x, σ_y and τ_{xy}) must be interpolated in the domain of every finite element using its shape functions. Next, the principal stresses σ_a and σ_b must be calculated at every pixel of the digital image associated to a corresponding point of the finite element structure. When this is done, the last step is to calculate the greyscale intensity of the pixel under consideration (Eq. (3)). One may vary the value of constant C which determines the density of fringes in the digital image.

The readers can experiment with different structures. Of course, the most fascinating results are produced when the structures contain singular points or regions with concentrated stresses. Disks and rings in diametral compression, plates with notches or small holes in compression or bending modes are just few examples of interesting objects. Three-dimensional or full-colour photoelasticity can produce even more pictorial computational effects but is out of scope in this paper.

References

[1] National Research Council. Research directions in computational mechanics. A report of the United States National Committee on Theoretical and Applied Mechanics. Washington, DC: National Academy Press; 2000.

[2] Kobayashi AS. Handbook on experimental mechanics. Bethel: Society for Experimental Mechanics Inc.; 1993.

[3] Chandrashekhara K, Antony SJ. An experimental–numerical hybrid method for elastic contact problems. Mechanics of Structures and Machines 1994;22:487–504.

[4] Fujikawa M, Takashi M. An experimental and numerical hybrid technique for reconstructing boundary conditions in elastic analysis. Journal of Strain Analysis for Engineering Design 2007;42:47–54.

[5] Dally JW, Riley WF. Experimental stress analysis. New York: McGraw-Hill; 1991.

[6] Asundi A, Sajan MR. Multiple LED camera for dynamic photoelasticity. Applied Optics 1995;34:2236–40.

[7] Pacey MN, Haake SJ, Patterson EA. A novel instrument for automated principal strain separation in reflection photoelasticity. Journal of Testing and Evaluation 2000;28:229–35.

[8] Bathe KJ. Finite element procedured in engineering analysis. Englewood Cliffs, NJ: Prentice-Hall; 1982.

[9] Ramesh K, Pathak PM. Role of photoelasticity in evolving discretization schemes for FE analysis. Experimental Techniques 1999;23:36–8.

[10] Ragulskis M, Palevicius A, Ragulskis L. Plotting holographic interferograms for visualization of dynamic results from finite-element calculations. International Journal for Numerical Methods in Engineering 2003;56:1647–59.